

Effect of Metal Vapor on Thermal Plasma in Gas Tungsten Arc Welding

Kentaro Yamamoto¹, Manabu Tanaka¹, Shinichi Tashiro¹, Kazuhiro Nakata¹,
Keiichi Suzuki², Anthony B. Murphy³ and John J. Lowke³

¹ *Joining & Welding Research Institute, Osaka University
11-1 Mihogaoka, Ibaraki, Osaka 567-0047, Japan*

² *Kobe Steel, LTD.
100-1 Miyamae Fujisawa, Kanagawa 255-8551, Japan*

³ *CSIRO Industrial Physics
P.O. Box 218, Lindfield NSW 2070, Australia*

Abstract

A gas tungsten arc in helium is modeled taking into account the contamination of the plasma by the metal vapor from the weld pool surface. The whole region of gas tungsten arc welding is treated using a unified numerical model. A viscosity approximation is used to express the diffusion coefficient in terms of the viscosities of the helium gas and the iron vapor. The time-dependent two-dimensional distributions of temperature, velocity and iron vapor concentration are predicted, together with the weld penetration as function of time for a 150 A arc at atmospheric pressure. It is shown that the thermal plasma in gas tungsten arcs is markedly influenced by iron vapor from the weld pool surface and that the concentration of the iron vapor in the plasma is dependent on temperature of the weld pool surface.

Keywords: Simulation, Arc, Welding, Metal vapor.

1. Introduction

During the arc welding process, four states of matter, solid, liquid, gas and plasma, simultaneously exist and mutually interact within a volume of only 1 cm³. The temperature range is wide, ranging from about 20 000 K in the arc plasma, about 3000 K in the tungsten cathode, about 2000 K in the molten steel, down to room temperature in the surrounding regions (Tanaka, et al, 2006). Due to the remarkable progress in computer simulation and observation techniques recently, it has become possible to understand the phenomena in arc welding processes quantitatively (Fan, et al, 2004 and Nishiyama, et al, 2006). However, it has not been possible to accurately predict the welding parameters, such as the arc voltage and the weld geometry. It is known empirically that the arc voltage in gas tungsten arc (GTA) on water-cooled copper differs from that in GTA welding. This phenomenon is caused by the metal vapor from the weld pool surface. For a full understanding and accurate prediction of these

parameters, it is necessary to understand the behavior of metal vapor in the arc plasma.

Metal atoms generally have more low-energy excited states, and are more easily ionized, than atoms of shielding gases such as argon and helium. These characteristics contribute to an increase of the radiative emission coefficient and the electric conductivity of the plasma. It is estimated that the former affects the thermal pinch effect and the energy efficiency of the arc plasma and that the latter affects the current density distribution. Tashiro et al conducted a virtual experiment by numerically simulating a pure helium arc and an arc in helium uniformly mixed with 30 mol% iron atoms (Tashiro, et al, 2007), and showed that an obvious arc constriction occurred for the latter case. Their results suggested that existence of metal vapor changed the heat source property in the arc welding process.

As noted above, there have been significant advances in the simulation of the arc welding. For example, a numerical simulation of gas metal arc welding, including the formation of droplets from a steel wire electrode, has been reported (Fan, 2004).

However, the welding gas was pure argon, and the effect of metal vapor was not considered. On the other hand, calculations of the behavior of metal vapor in an atmospheric pressure plasma have also been reported (Menart, 1999). However, the conditions were far from those of welding because a solid electrode with constant temperature was assumed. It is important for accurate understanding of the arc welding process to consider the mixing of the metal vapor in a model that takes into account the tungsten cathode, the arc plasma and the weld pool.

In the present paper, a numerical model of stationary GTA welding taking into account the iron vapor produced from the weld pool surface is used, and the distribution of the metal vapor, the plasma temperature and the formation of the weld pool in GTA welding are simulated.

2. Simulation model

The tungsten cathode, arc plasma and anode are described relative to cylindrical coordinates, assuming rotational symmetry around the arc axis. The radius of calculation domain is 25 mm and the height is 45 mm (cathode: 30 mm, arc gap: 5 mm, anode: 10 mm). The diameter of the tungsten cathode is 3.2 mm with a 60 degrees conical tip. The anode is of water-cooled copper or stainless steel. Helium shielding gas is introduced from the outside of the cathode on the upper boundary at the flow rate of 30 L/min.

The convection in the weld pool is influenced by the shear stress due to the convective flow of the cathode jet, the Marangoni force due to the gradient in the surface tension of the weld pool, buoyancy due to gravity and the electromagnetic pinch force due to the arc current. Only the driving forces of the weld pool convection at the boundary between the weld pool and the arc plasma are explained here. First, the shear stress is already included in radial momentum conservation through the viscosity at the anode surface. Second, the Marangoni force is given by

$$M_A = \frac{\partial}{\partial z} \left(\frac{\partial \gamma}{\partial T} \frac{\partial T}{\partial r} \right) \quad (1)$$

(Tanaka, et al, 2007) where T is temperature, γ is the surface tension of the weld pool. In this paper, stainless steel is assumed to have low sulfur content (about 10 ppm) and the variation of the surface tension at the weld pool surface is assumed to decrease linearly with increasing temperature ($\partial \gamma / \partial T = -0.46 \text{ mN/mK}$) (Tanaka, et al, 2007).

A species conservation equation expressed by Equation (2) is applied to take into account the metal vapor behavior (Menart, 1999). In practice, metal vapor species in an arc plasma with a stainless steel

anode include Fe, Cr, Mn and so on (Terasaki, et al, 2002). However, to simplify the model and facilitate calculation, only iron vapor is considered in this model.

$$\begin{aligned} \frac{\partial}{\partial t} (\rho C_1) + \frac{1}{r} \frac{\partial}{\partial r} (r \rho v_r C_1) + \frac{\partial}{\partial z} (\rho v_z C_1) \\ = \frac{1}{r} \frac{\partial}{\partial r} \left(r \rho D \frac{\partial C_1}{\partial r} \right) + \frac{\partial}{\partial z} \left(\rho D \frac{\partial C_1}{\partial z} \right) \end{aligned} \quad (2)$$

where t is time, v_r and v_z are the radial and axial velocities, ρ is the density, C_1 is mass fraction concentration of iron vapor and D is the binary diffusion coefficient, which is expressed by the viscosity approximation equation:

$$D = \frac{2\sqrt{2}(1/M_1 + 1/M_2)^{0.5}}{\left\{ (\rho_1^2 / \beta_1^2 \eta_1^2 M_1)^{0.25} + (\rho_2^2 / \beta_2^2 \eta_2^2 M_2)^{0.25} \right\}^2} \quad (3)$$

where M_1 and M_2 are the molecular weights of iron and the shielding gas respectively. Similarly, ρ_1 , ρ_2 , η_1 , η_2 are respectively the density and viscosity of iron and the shielding gas. β_1 , β_2 are the dimensionless constant defined as $\beta_i = (D_{if} \rho_i) / \eta_i$, and theoretically range 1.2 to 1.543 for various species of gas, such as Ar, He, H₂, N₂, O₂, CO₂ and so on. It is assumed that $\beta_1 = \beta_2 = 1.385$, which is based on the mean value of experimental data (Wilke, 1950). The viscosity approximation is not strictly justified since it does not take into account ionized species and is at best reasonably accurate (Murphy, 1996); however it is considered to be a useful first approximation for the arc welding model.

C_1 is set to be zero in the cathode area and in the solid area of the anode. However, at the anode surface where the temperature is above the melting point, C_1 is set to:

$$C_1 = \frac{p_{v,1} M_1}{p_{v,1} M_1 + (p_{atm} - p_{v,1}) M_2} \quad (4)$$

(Menart, 1999) where p_{atm} is atmospheric pressure and $p_{v,1}$ is the iron vapor partial pressure, which is a function of the weld pool temperature. According to Equation (4), C_1 has values between zero and 1.0. ($\partial C_1 / \partial r = 0$ at the arc axis. For other boundary conditions, $C_1 = 0$).

In the present model, plasma properties are dependent on not only the temperature but also the mole fraction of iron vapor. Plasma properties at intermediate concentrations of iron vapor are calculated using a linear approximation based on the properties at 0 mol%, 1 mol%, 10 mol%, 20 mol% and 30 mol% (Murphy, 1995). The properties were

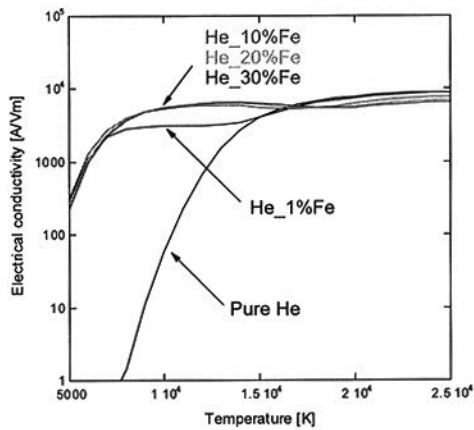


Fig. 1 Dependence of electrical conductivities of helium gas on temperature for each mixing ratio..

calculated assuming the arc plasma to be in the local thermodynamic equilibrium (LTE), and using the Chapman-Enskog approximation. For example, the electrical conductivities, which are significantly affected, are shown in Figure 1. The electrical conductivities are greatly increased by the addition of iron vapor at temperatures below 15 000 K, and the values for mixing ratios 1%, 10%, 20% and 30% are almost the same.

The other approximations, governing equations and boundary conditions are given in detail in the previous paper (Tashiro, et al, 2007). The governing and auxiliary equations are solved iteratively by the SIMPEC numerical procedure.

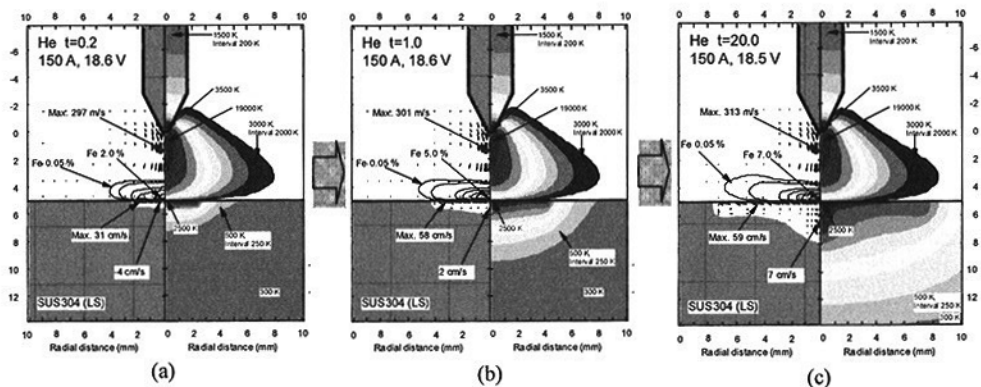


Fig. 2 Calculated results for helium GTA welding for 150 A at (a) 0.2 s, (b) 1.0 s and (c) 20 s after arc ignition.

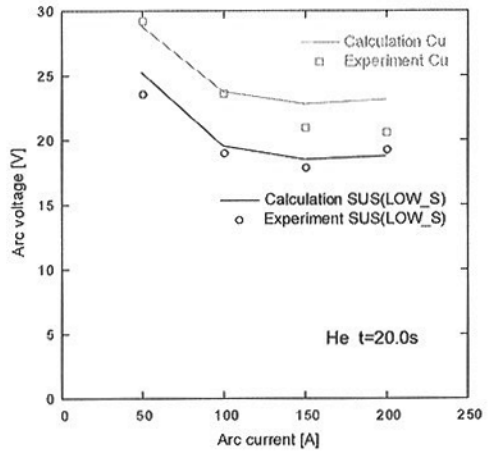


Fig. 3 Comparison of calculated arc voltage with experimental results.

3. Calculation results

The present model is applied to the case of stationary helium GTA welding of stainless steel. Figure 2 shows the two-dimensional distributions of temperature, fluid flow velocity and mole fraction of iron vapor at a time (a) 0.2 s, (b) 1.0 s and (c) 20 s after arc ignition. The distribution of iron vapor depends of the diffusion term and the convection term, as described in Equation (2). Due to the cathode jet, which leads to flow velocities of 300 m/s in the welding arc, the convection term has a strong effect. Therefore, it is found that distribution of iron vapor expands in the radial direction and is concentrated around the weld pool surface. At 20 s after arc ignition, the concentration of iron vapor in

the arc plasma is up to 7 mol%, which is in good agreement with the experimental data presented in (Terasaki, 2002).

Figure 3 shows calculated values of arc voltage for 50 A, 100 A, 150 A and 200 A arc current. Experimental results are also shown (the calculated results are represented by lines and the experimental results by symbols). Arc voltages for a water-cooled copper anode and a stainless steel anode are shown; in the case of stainless steel, arc voltages are again shown at 20 s after arc ignition. The experiment is consistent with the calculation. The work piece is SUS304 stainless plate (50 mm×100 mm×10 mm thick) with 10 ppm sulfur content mounted on a water-cooled copper plate. The welding conditions, such as arc length, electrode diameter and flow rate of shielding gas, are the same as the conditions of the calculation. Figure 3 shows that the arc voltages for the stainless steel anode are about 5 V lower than those for the water-cooled copper anode at any arc current. This is due to the effect of iron vapor from the weld pool. As shown in Figure 1, even a small amount of iron vapor increases the electrical conductivity. Consequently, the arc voltage decreases because of the lower voltage gradient, particularly just above the weld pool. Between 100 and 200 A, a difference of 2 to 3 V is founded between calculation and experiment in the case of water-cooled copper anode. A likely reason for this difference is that a small amount of copper vapor is produced from the anode surface at high current, for which the heat input density is large, this decreasing the voltage in the experiments.

4. Conclusions

A numerical model of a stationary GTA welding taking into account the iron vapor from the weld pool surface has used, and the effect of the iron vapor on the properties of the arc and the weld pool has simulated. The main conclusions are summarized as follows:

- (1) Due to the cathode jet velocity of 300 m/s in the welding arc, the convection term strongly affects the distribution of the iron vapor. It was found that iron vapor expanded mainly in the radial direction and remained concentrated around the weld pool surface.
- (2) Calculated values of arc voltage were in good agreement with experimental results, and the arc voltage for a stainless steel anode was clearly lower than that for a water-cooled copper anode.

Acknowledgment

This work is supported by a grant-in-aid for Scientific Research (B) (2007) from the Japan Society for Promotion of Science (JSPS).

References

- Fan, H. G. and R. Kovacevic (2004): *J. Phys. D*, 37, p2531-2544.
- Menart, J. and L. Lin (1999): *Plasma Chem. & Plasma Process.*, 19-2, p153-170.
- Murphy, A. B. (1995): *Plasma Chem. & Plasma Process.*, 15-2, p279-307.
- Murphy, A. B. (1996): *J. Phys. D*, 29, p1922-1932.
- Nishiyama, H., T. Sawada, H. Takana, M. Tanaka and M. Ushio (2006): *ISIJ Int.*, 46-5, p705-711.
- Tanaka, M., T. Watanabe, T. Isa and H. Nishiwaki (2006): *J. Plasma & Fusion Res.*, 82-8, p492-496 (in Japanese).
- Tanaka, M. and J.J. Lowke (2007): *J. Phys. D*, 40, p1-23.
- Tashiro, S., M. Tanaka, K. Nakata, T. Iwao, F. Koshiishi, K. Suzuki and K. Yamazaki (2007): *Sci. Technol. Weld. Join.*, 12-3, p202-207.
- Terasaki, H., M. Tanaka and M. Ushio (2002): *Quarterly J. Japan Welding Soc.*, 20-2, p201-206 (in Japanese).
- The Japan Institute of Metals (1993): *Edition No. 3 Data Book of Metals*; Tokyo, MARUZEN CO., LTD (in Japanese).
- Wilke, C. R. (1950): *J. Chem. Phys.*, 18-4, p517-519.